IMPACT OF LAND USE AND CLIMATE CHANGES ON FLOOD INUNDATION AREAS IN THE LOWER CIMANUK WATERSHED, WEST JAVA PROVINCE

Muhammad Ardiansyah[1,3)]*, Rifqi Aditya Nugraha[2)], La Ode Syamsul Iman[1)], and Syamsu Dwi Djatmiko[3)]

[1)] Department of Soil Sciences and Land Resources, Faculty of Agriculture, IPB University, Jl. Meranti – Kampus IPB Dramaga, Bogor, West Java 16680
[2)] Undergraduate Student at Department of Soil Sciences and Land Resources, Faculty of Agriculture, IPB University, Jl. Meranti – Kampus IPB Dramaga, Bogor, West Java 16680
[3)] Center for Climate Risk and Opportunity Management in Southeast Asia and Pacific, IPB University, Jl. Pajajaran – Kampus IPB Baranangsiang, Bogor, West Java 16143

ABSTRACT

Land use and climatic changes potentially affect the surface runoff and inundation in watershed zones. Every year, the outflow of the Cimanuk River causes floods across the majority of the upper area as well as the lower area of the Cimanuk Watershed. This study aimed to assess the impact of climatic and land use changes on future flood inundation in the Lower Cimanuk Watershed using a Rainfall-Runoff Inundation model. Land-use change has been prepared for modeling using a multi-layer perceptron neural network and Markov Chain approach, while climate change was modelized by using HadGEM2-ES global climate model data under scenarios RCP4.5. Result of the research indicate that the forest area was projected to decline in this watershed zone, from 19.54% of the total area in 2019 to 17.73% in 2050. Similarly, the area of paddy fields was predicted to decline from approximately 34.36% in 2019 to 29.65% in 2050. In contrast, other types of land use such as dryland agriculture, mixed dryland agriculture, and settlements were projected to increase in the future. The coverage of the simulated flood inundation area using the Rainfall-Runoff Inundation model was estimated to reach 179.4 km^2 in 2019. The simulation results showed an increase in flood inundation areas in 2030 and 2050, alongside changes in land use and climate. The areas affected by flood inundation were estimated to reach 253.3 km^2 in 2030. This coverage was expected to increase by 311.9 km^2 in 2050, with severely affected land uses including settlements, dry land agriculture, mixed dry land agriculture, paddy fields, and ponds.

Key words: inundation simulation, land use change and modelling, RRI model

INTRODUCTION

Climate-related disasters such as floods, hurricanes, droughts, and heat waves have increased worldwide (Thomas and López, 2015), including in Indonesia. In particular, flooding is a hydrometeorological disaster that often occurs in Indonesia (Asdak *et al.*, 2018; Narulita and Ningrum, 2018). Data from the National Disaster Management Agency (BNPB) has shown that 784 floods occurred in 2019. That number increased to 1,080 in 2020, making floods the most frequent natural disaster nationally, resulting in serious social, economic, and environmental impacts (BNPB, 2019; BNPB, 2020). The dynamics of the earth's surface water in recent periods, marked by the onset of extreme situations, have become one of the main causes of flooding disasters. As a result of these water patterns, extreme wet rains occur more frequently, which then lead to the flooding of lowland areas due to surface runoff and the spilling of water from riverbeds (Húska *et al.*, 2017). In the case of a watershed, flooding occurs when the watershed system receives an unusually high rainfall intensity or experiences a prolonged rainfall event that leads to an excess streamflow rate beyond the channel capacity (Dingman, 1994).

Land use/cover change and climate variability/change are two major factors controlling streamflow fluctuation and increased rainfall (Boer and Faqih, 2004; Naylor *et al.*, 2007; Berihun *et al.*, 2019; Tarigan and Faqih, 2019). Land cover and use changes have been widely recognized to pose a threat to water reservoirs and watershed management by increasing the intensity of surface runoff (Chow *et al.*, 1988; Woldemichael *et al.*, 2012; Yigzaw and Hossain, 2016). Global warming, resulting from an increased concentration of greenhouse gases in the atmosphere, will also cause a rise in temperatures. Moreover, rainfall is expected to vary considerably by region and may become more extreme (IPCC, 2017; Thomas and López, 2015). In addition, climate change can significantly impact water resources by affecting the hydrological process. The changes in temperature and rainfall can directly affect the quantities of evapotranspiration and runoff components (Alerts and Droogers, 2004). In the district of Indramayu, climate change was projected to cause an increase in temperature by up to 4 ºC, a decline in rainfall during the dry season, and an increased intensity of rainfall during the rainy season (Faqih *et al.*, 2016). The increased rainfall in the rainy season may impact the flooding in watersheds. Thus land cover or use changes, when combined with climate change, may increase the risk of flooding in watersheds, potentially resulting in increased flood events in the future.

Therefore, to prevent and mitigate flood damage, it is important to understand the characteristics of floods and their changing patterns as a consequence of changes in land use and climatic events. Many studies have been conducted to distinguish the roles of land use and climate change in water resources (He, 2013). In Indonesia, however, several studies have focused on the impact of land use and climate change on hydrological processes. For example, Kudo *et al.* (2015) and Nastiti *et al.* (2016) quantitatively measured the impacts of land use and climate change on flood risk changes in the Citarum Watershed and Solo Watershed

*) *Corresponding author: Telp. +62811112973; Email. ardysaja@gmail.com* *DOI: http://dx.doi.org/10.29244/jitl.23.2.53-60*

respectively. They found that the inundation areas under future climates are expected to be larger than those produced by the present climate events. In other studies, the impacts of both climate and land use changes were shown to cause an increase in the maximum peak discharge in the Merangin Tembesi Watershed (Tarigan and Faqih, 2019) as well as an increase in runoff and a decline in base flow contribution to annual streamflow in the Cimanuk Watershed (Ridwansyah *et al.*, 2020).

The hydrological models used to analyze the impact of land use change and climate change on the water balance in the above studies were process-based approaches using the Soil and Water Assessment Tool (SWAT) and Rainfall-Runoff Inundation (RRI) models. Such a process-based approach requires more data as input and has a high level of uncertainty in the context of parameter estimation (Xu *et al.*, 2014; Zhang *et al.*, 2016). The SWAT hydrological model can validate and correlate the relationship between surface water and groundwater using the principle of water equilibrium, along with estimating the consequences of possible changes (Ridwansyah *et al.*, 2020). The RRI model can simultaneously simulate the runoff within reach of the river and the inundation over the floodplain, in order to analyze discharge and inundation in the watershed (Sayama *et al.*, 2012). This model also works well in areas that often experience a shortage of hydrological data, including mountainous regions. In this context, this approach uses satellite-based rainfall data to estimate the flood runoff and inundation at the watershed scale (Sayama *et al.*, 2015; Nastiti *et al.*, 2016). The objective of this study is to analyze the impact of changes in climate and land use on the future flood inundation areas in the Lower Cimanuk Watershed.

MATERIALS AND METHODS

Study Site

The study site was located in the Lower Cimanuk Watershed, West Java Province, Indonesia. It is a part of the Cimanuk Watershed with an area of 4,011 km^2, located in the northern part of Java Island. Most of the downstream sections of the watershed system are located within the administrative districts of Indramayu and Cirebon, as shown in Figure 1. The watershed is experiencing rapid land use change that has led to an increase in surface runoff (Ridwansyah, 2012).

Data Collection

We used the RRI hydrological model to calculate the flood inundation area and procedures to estimate the flood inundation area can be found in Sayama *et al.* (2017). The input data for the RRI model included the Digital Elevation Model HydroSHEDS based on the Shuttle Radar Topography Mission data with a grid size of 30 arc seconds or approximately 919 x 919 m^2; flow accumulation and flow direction derived from HydroSHEDS; soil data from global data sets available in the model; land use of 2000 and 2015 from the Ministry of Environment and Forestry; land use of 2019 from Landsat 8-OLI; and streamflow discharge data from Monjot Station belonging to Balai Besar Wilayah Sungai of Cimanuk-Cisanggarung (Ministry of Public Works and Housing). In addition, we used the daily global climate data set from the Climate Hazards Group Infrared Precipitation with Station (CHIRPS) data (Funk *et al.*, 2014). CHIRPS provides a global rainfall data set that has been corrected with the observational rainfall data. The correction method uses a quantile mapping approach (Piani *et al.*, 2010), following the procedures of Jadmiko *et al.* (2017). This rainfall data has a grid size of 0.5 degrees, so there were 224 grids in the study area. Flood assessment was conducted from April 1 to April 30 in 2019 as a baseline (BAU) scenarios, representing the recorded flood event in the Lower Cimanuk Watershed in 2019.

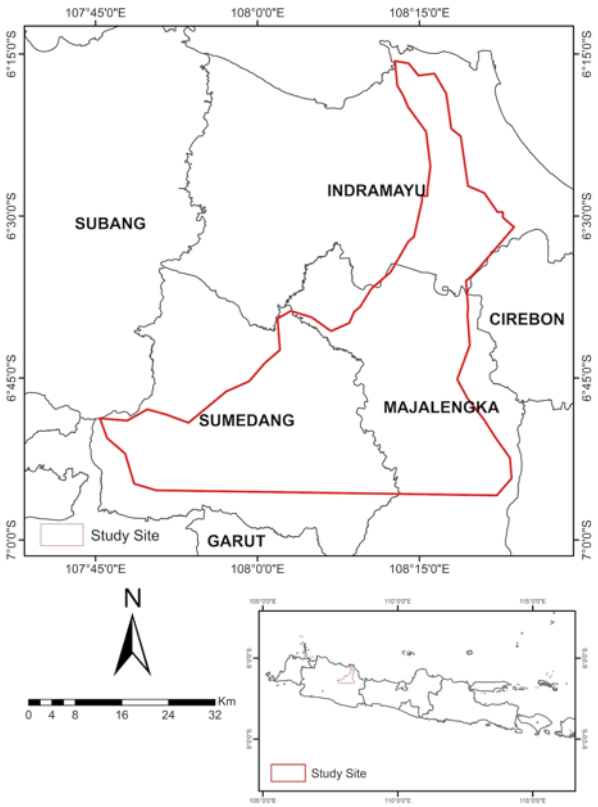

Figure 1. Study site in West Java Province, Indonesia

Climate Change Scenario

The assessment of climate change was based on the emissions projection under the Representative Concentration Pathway (RCP) 4.5 scenario (Moss *et al.*, 2010). Although there are many alternative scenarios, the application of RCP4.5 provides a common platform for climate models to explore climate system responses to stabilize the anthropogenic component of radiation forcing (Thomson *et al.*, 2011). Climate change projection was simulated using the nonhydrostatic regional climate model RegCM (RegCM4). The scheme and simulation process of RegCM4 are explained in Faqih *et al.* (2016). The model was run with a spatial resolution of 20 x 20 km^2 using initial conditions and boundary conditions (ICBC) data, the output of the HadGEM2-ES global climate model (Collins *et al.*, 2011). The outputs of RegCM4 were corrected following the procedures from Jadmiko *et al.* (2017) using the quantile mapping approach (Piani *et al.*, 2010).

Land Use Change

Land use change was analyzed using 2000 and 2015 land use maps whose accuracy was assessed using Landsat 7 ETM+ images, Landsat 8-OLI images and ground truth. Land use predictions for 2030 and 2050 were based on the historical trends of land use change for the period 2000–2015, which were modeled in the Land Change Modeler on Idrisi software using the multi-layer perceptron (MLP) neural network and Markov Chain (MC) modeling. This approach involved change analysis, transition potential, and change prediction. The change analysis was used to assess changes (i.e., area gains and losses) between the land use in 2000 and that in 2015, applying transition potential modeling and change prediction to represent the time range between these two years. With the application of four variables, i.e., distance from roads, distance from rivers, population density, and slope, each transition created by the change analysis was then used as a sub-model. Transition potentials were modeled by a back propagation learning algorithm using the MLP. In order to conduct a land use change prediction, the MC modeling was applied with the predicted years of 2019 for validation, 2030, and 2050 using all potential transition sub-models (Eastman, 2012). The validation, based on the kappa value, was used to measure the suitability of the 2019 land use prediction, with the observed 2019 land use for comparison drawn from the visual interpretation of Landsat 8-OLI. The types of land use are the same as those in the 2000 and 2015 land use maps from the Ministry of Environment and Forestry based on SNI 2010:7645 (BSN, 2010).

Model Calibration

Model calibration was conducted to evaluate the effectiveness of the simulation in the model. To evaluate the performance of the RRI model with respect to the simulated and observed discharges, we used a simple Nash-Sutcliffe Efficiency (NSE) statistic. The NSE is a normalized statistic that determines the relative magnitude of the residual variance compared to the measured data variance (Nash and Sutcliffe, 1970). The parameters used for the calibration were the observed discharge (Q_obs) and simulated discharge (Q_sim), formulated as follows:

$$NSE = 1 - \left[\frac{\sum(Q_{obs\,i} - Q_{sim\,i})^2}{\sum(Q_{obs\,1} - \bar{Q}_{obs})^2}\right]$$

where Q_obs is the observed discharge (m^3/s), $\bar{Q}$_obs is the average observed discharge ($m^3\ s^{-1}$), and Q_sim is the simulated discharge ($m^3\ s^{-1}$).

RESULTS AND DISCUSSION

Land Use Change Assessment

The land use in the research location in 2000, 2015 and 2019 resulting of visual interpretation of Landsat 8-OLI images consisted of 9 classes, namely water body, forest, settlement, plantation, dryland agriculture, mixed dryland agriculture, paddy field, ponds and bare land, with an accuracy of a kappa value of 0.95, 0.92 and 0.90 respectively. The performance of LCM was excellent, with a kappa value of 0.94. This meant that land use projections could be made for 2030 and 2050. The land use maps for the years 2019, 2030, and 2050 are presented in Figure 2. Additionally, the changes for each land use category are summarized in Table 1. In 2019, the land use in the Lower Cimanuk Watershed was dominated by paddy fields, which covered approximately 34.36% (658.54 km^2) of the total area. This was followed by the forest area, covering around 20.78% (398.25 km^2) of the total area. Following this were five types of land use, as follows: dryland agriculture 19.55% (374.61 km^2), mixed dryland agriculture 11.23% (215.21 km^2), settlements 9.56% (183.22 km^2), ponds 2.25% (43.17 km^2), and plantations 1.4% (26.89 km^2). Meanwhile, water bodies and bare land were estimated to cover less than 1% of the total area. Paddy fields are found in the northern and central parts of the watershed, most of which belong to the Indramayu District. This is understandable due to the important role of the Indramayu District as a producer of rice in West Java. Between 2030 and 2050, paddy fields and forests were predicted to remain the two most dominant land uses in the Lower Cimanuk Watershed, although they were projected to experience decreases of 7.11% and 5.97% respectively by 2030, and further decreases of 13.70% and 14.68% respectively by 2050.

In contrast, dryland agriculture, mixed dryland agriculture, settlements, bare land, and plantations were expected to increase in 2030 and 2050. The largest increase was predicted to occur in the case of dryland agriculture, from around 13.04% in 2030 to 25.91% in 2050. This increase was predicted to partly derive from forest conversion. Forests are generally located in the south-central part of the watershed; between 2019 and 2050, this area will be deforested at a rate of approximately 1.99 km^2 per year. The forest area was projected to decline from 19.54% of the total area in 2030 to only 17.73% in 2050. The expansion of settlements and agricultural lands in the northern and southern parts of the watershed, along with deforestation activities, are expected to be the driving factors that affect the hydrological processes and potentially increase the runoff (He *et al.*, 2013).

Performance of the RRI model

Streamflow calibration based on the daily model shows reasonably good agreement between the simulated and observed discharge values (Figure 3). The blue line represents discharge ($m^3\ s^{-1}$) recorded at the Monjot Station, while the red line represents discharge simulated by the RRI model. The green bar graph shows the daily rainfall (mm), which was derived from the CHIRPS data. The peak of the discharge was seen on 8–9 April 2019, which was the date of flooding in the Indramayu District. This result shows that the RRI model performed well, with an NSE value of 0.66 (Moriasi *et al.*, 2007). Thus, the model was suitable for simulating the relative impacts of land use change and climate change on the flood inundation areas in the Lower Cimanuk Watershed. We simulated four scenarios for future conditions: a) the impact of land use change in 2030 (LU30), b) the impact of land use change in 2050 (LU50), c) the combined impact of land use and climate change in 2030 (LU-CC30), and d) the combined impact of land use and climate change in 2050 (LU-CC50).

Impact of Changes in Land Use and Climate on Inundation Area

In addition to streamflow discharge, the RRI model simulates the water depth (m) on the slopes and inundation areas. Figure 4 shows the results obtained from the simulations of flood inundation using RRI, which were affected by land use changes. There are five scenarios in this simulation. In all scenarios, the climate input parameter used was based on the 2019 data. Similarly, the input parameters of land use categories used in the model were based on the 2019 data (BAU), as well as 2030 and 2050 land use maps (Table 1). The results of the BAU simulation show a flow depth of 1 m (Table 2). This finding is in agreement with the flood event that occurred in April 2019 with a flow depth of 1 m. The flood submerged 5 sub-districts including 8,271 houses and affected more than 20,000 people. The coverage of simulated flood inundation areas reached 179.4 km^2, which was spread across several areas of the watersheds, predominantly those located in the Indramayu District. There was no information on the extent of the impact of flooding in that month, the simulated inundation area may be overestimated because the observation data used in the model is limited. In addition, the spatial resolution of DEM used in the model was also low (0.5 degree). However, several studies have demonstrated that the RRI model tends to underestimate the flood inundation area at the watershed scale (Sayama *et al.*, 2015; Nastiti *et al.*, 2016). The simulation of the LU30 scenario predicted an increase in the coverage of flood inundation areas to 249.8 km^2 in 2030. Under this scenario, settlements, paddy fields and ponds were three of the most affected land use types. Meanwhile, in the simulated LU50 scenario, whereby the forest area was lower than that in the LU30, and the areas affected by flood inundation extended to 262.9 km^2, most affecting the land use types of settlements, agricultural land, paddy fields, and ponds. The increase in the coverage of flood inundation areas was mainly caused by factors related to land degradation, such as lower soil infiltration and increased runoff due to the decrease of forest area, both upstream and downstream of the watershed. A low infiltration rate will increase the surface runoff component and, in turn, will also increase the peak discharge (Tarigan and Faqih, 2019). The simulation results of this model show the strong impact of land use change on the hydrological process in the Lower Cimanuk Watershed. These results confirm the findings from several previous studies (Nugroho *et al.*, 2013; Ridwansyah *et al.*, 2020).

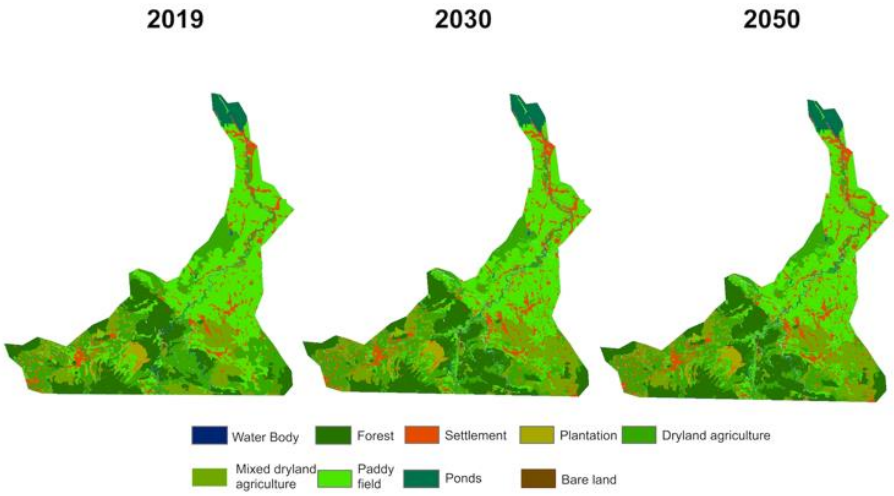

Figure 2. Land use maps for 2019, 2030, and 2050 in the Lower Cimanuk Watershed

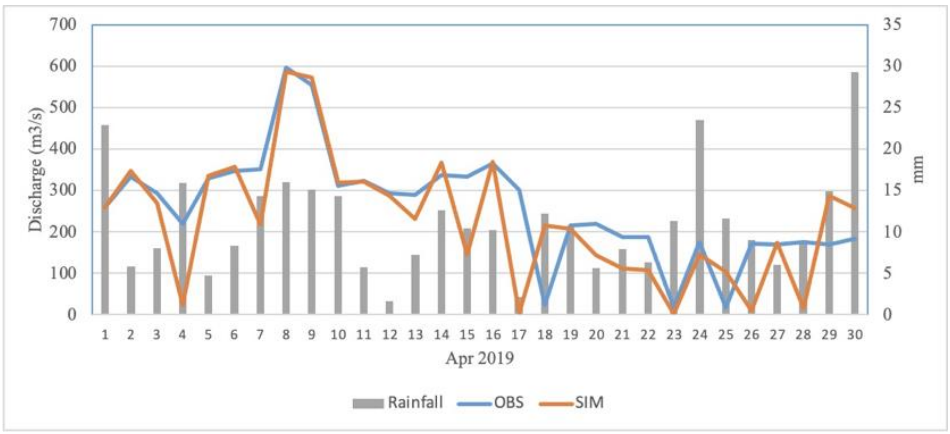

Figure 3. Comparison of observed and simulated discharge in the Lower Cimanuk Watershed

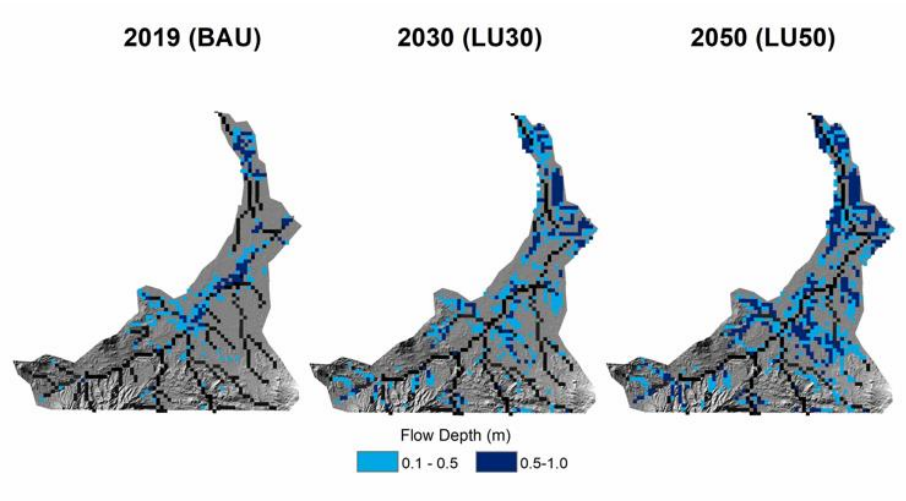

Figure 4. Simulated inundation area based on land use change scenarios

Table 1. Changes in areas of land use in 2019 (baseline), 2030, and 2050

Land use	2019		2030		2050		% of change	
	km^2	%	km^2	%	km^2	%	2019 - 2030	2019 - 2050
Water body	14.03	0.73	14.03	0.73	14.03	0.73	0.00	0.00
Forest	398.25	20.78	374.46	19.54	339.77	17.73	-5.97	-14.68
Settlement	183.22	9.56	199.74	10.42	226.27	11.81	9.02	23.50
Plantation	26.89	1.40	27.14	1.42	27.14	1.42	0.93	0.93
Dryland agriculture	374.61	19.55	423.45	22.09	471.68	24.61	13.04	25.91
Mixed dryland agriculture	215.21	11.23	220.22	11.49	223.51	11.66	2.33	3.86
Paddy field	658.54	34.36	611.71	31.92	568.35	29.65	-7.11	-13.70
Ponds	43.17	2.25	43.17	2.25	43.17	2.25	0.00	0.00
Bare land	2.64	0.14	2.64	0.14	2.64	0.14	0.00	0.00
Total	1,916.56	100.00	1,916.56	100.00	1,916.56	100.00		

Table 2. Flow depth, potential flood inundation areas, and affected land uses due to land use change

Flow Depth (m)	Inundation Areas (km2)			Affected Land Uses
	2019 (BAU)	2030 (LU30)	2050 (LU50)	
0.1 - 0.5	102.7	134.9	138.5	Settlements, dry land agriculture, mixed dry land agriculture, paddy fields, ponds
0.5 - 1.0	76.7	114.9	124.4	Settlements, mixed dry land agriculture, paddy fields, ponds
Total	179.4	249.8	262.9	

The impact of both land use and climate change is shown in Figure 5 and Table 3. In all scenarios, both land use and climate input parameters for the RRI model were adjusted simultaneously. We used the maximum daily rainfall from climate change data for the years of 2030 to 2050. The simulations of LU-CC30 and LU-CC50 scenarios showed an increase in the inundation areas in comparison with the previous scenarios. In particular, the inundation area in the LU-CC30 scenario was predicted to be larger than that in the LU30 scenario. The combined impact of land use and climate change was predicted to cause an expansion of flood inundation areas by 3.5 km^2 in 2030 relative to the LU30 scenario, in which climate change was not considered. The predicted increase in the inundation area was even greater when the combined impacts of land use change and climatic changes were simulated using the RRI model. The flood inundation area was predicted to increase by 49.0 km^2 compared to the scenario of no climate change (LU50), while the most affected land uses were settlements, agricultural land, paddy fields, and ponds. This demonstrates that land use and climate change can affect the future extent of flood inundation. However, since the increase in the flood inundation areas due to the combined impact of both land use and climate changes did not exceed the single impact of land use change, it appears that land use change has a stronger impact on flood runoff and inundation than climate change. Other studies have also shown that land use change tends to exert stronger impacts than climate change (Xu *et al.*, 2014; Mwangi *et al.*, 2016).

The findings of this study confirm that land use and climatic changes are the main drivers that can potentially alter the future streamflow discharge. This, in turn, will also affect the future flood runoff and inundation. Therefore, better and earlier identification of the impactful characteristics of land use and climate change on flood runoff and inundation will enable governments to select policies and prioritize actions for watershed management. As a long-term measure to reduce surface runoff and increased infiltration due to the reduction in forest coverage, critical lands in the upstream watershed need to be reforested and the remaining forest needs to be conserved in order to maintain water catchment areas. Reforestation programs and the preservation of forest areas are likely to reduce peak flood discharges to some extent and slightly reduce the peak discharge of a watershed (Szwagrzyk *et al.*, 2018). In addition, local communities must play a role in protecting forested areas. An introduction of good practices regarding the management of soil and water conservation measures in the agricultural sector for local communities is also necessary. These measures can help increase infiltration and reduce the rate of sedimentation in the watershed.

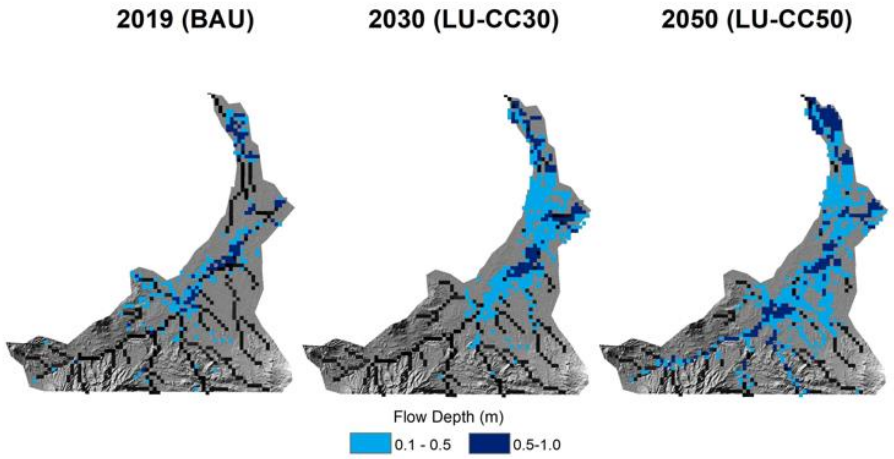

Figure 5. Simulated inundation area based on combined land use and climate change scenarios

Table 3. Flow depth, potential flood inundation areas, and affected land uses due to climate and land use changes

Flow depth (m)	Potential inundation areas (km^2)			Affected land uses
	2019 (BAU)	2030 (LU-CC30)	2050 (LU-CC50)	
0.1 - 0.5	102.7	134.3	187.3	Settlements, dry land agriculture, mixed dry land agriculture, paddy fields, ponds
0.5 - 1.0	76.7	119.0	124.6	Settlements, mixed dry land agriculture, paddy fields, ponds
Total	179.4	253.3	311.9	

CONCLUSIONS

The results of the RRI model show a reasonable performance with regard to the simulation of streamflow discharge in the downstream watershed, as indicated by the NSE value of 0.66 (classified as good). Despite using global climate data sets, the results of this study also confirm the capability of the RRI model to simulate the impacts of land use change and climate change on future flood inundation areas. Both changes have been shown to significantly impact future flood inundation areas. In this study, land use change was observed to have a greater impact on inundation areas than climate change. Nonetheless, with these two factors combined, the increase in flood area in the Lower Cimanuk Watershed will likely be higher in the future. As has been recommended by many previous studies, it is necessary to perform reforestation and protect against forest loss in the upstream watershed. It is also important to develop good practices with respect to soil and water conservation on the agricultural land in the downstream watershed.

ACKNOWLEDGMENTS

The authors would like to thank the Department of Soil Science and Land Resources, Faculty of Agriculture, and Center for Climate Risk and Opportunity Management in Southeast Asia and Pacific, IPB University, for facilitating the study.

REFERENCES

Alerts, J.C.H., and P. Droogers. 2004. Climate Change in contrasting river basins: adaptation strategies for water, food and environment. Walling: CABI.

Asdak, C., S. Supian, and Subiyanto. 2018. Watershed management strategies for flood mitigation: A case study of Jakarta's flooding. Weather and Climate Extremes, 21: 117–122.

Badan Standardisasi Nasional (BSN). 2010. Klasifikasi Penutup Lahan. Jakarta (ID): Badan Standardisasi Nasional [in Indonesia].

Berihun, M.L., A. Tsunekawa, N. Haregeweyn, D.T. Meshesha, E. Adgo, M. Tsubo, T. Masunaga, A.A. Fenta, D. Sultan, M. Yibeltal, and K. Ebabu. 2019. Hydrological responses to land use/land cover change and climate variability in contrasting agroecological environments of the Upper Blue Nile basin, Ethiopia. Science of the Total Environment, 689: 347–365.

Boer, R., and A. Faqih. 2004. An Integrated Assessment of Climate change Impacts, Adaptation and Vulnerability in Watershed Areas and Communities in Southeast Asia, Report from AIACC Project No. AS21 (Annex C, 95-126) International START Secretariat, District of Columbia, Washington.

Chow, V.T., D.R. Maidment, and L.W. Mays. 1988. Applied Hydrology. McGraw-Hill Book Company, New York, USA.

Collins, W.J., N. Bellouin, M. Doutriaux-Boucher, N. Gedney, P. Halloran, T. Hinton, J. Hughes, C.D Jones, M. Joshi, S. Liddicoat, G. Martin, F. O'Connor, J. Rae, C. Senior, S. Sitch, I. Totterdell, A. Wiltshire, and S. Woodward. 2011. Development and evaluation of an Earth-System model – HadGEM2. Geosci. Model Dev., 4(4), 1051-1075.

Dingman, S.L. 1994. Physical hydrology. MacMillan Publishing Co., New York, USA.

Eastman, J.R. 2012. IDRISI Selva manual and tutorial manual version 17. Clark University, Worcester, USA.

Faqih, A., R. Hidayat, S.D. Jadmiko, and Radini. 2016. Iklim historis dan skenario perubahan iklim di Indonesia: Analisis dan pemodelan iklim. United Nation Development Programme (UNDP), Kementrian Lingkungan Hidup dan Kehutanan (KLHK) [in Indonesia].

Funk, C.C., P.J. Peterson, M.F. Landsfeld, D.H. Pedreros, J.P. Verdin, and J.D. Rowland. 2014. A quasi-global precipitation time series for drought monitoring. U.S. Geological Survey Data Series (832), 4.

He, Y., K. Lin, and X. Chen 2013. Effect of Land Use and Climate Change on Runoff in the Dongjiang Basin of South China. Mathematical Problems in Engineering, 2013.

Húska1, D., L. Jurík, L. Tátošová, K. Šinka, and J. Jakabovičová 2018. Cultural landscape, floods and remote sensing. Journal of Ecological Engineering, 18 (3): 31–36.

Indonesian National Board for Disaster Management (BNPB). 2019. https://www.bnpb.go.id/infografis. [in Indonesia]

Indonesian National Board for Disaster Management (BNPB). 2020. https://www.bnpb.go.id/informasi-bencana. [in Indonesia]

Intergovernmental Panel on Climate Change (IPCC). 2017. Towards new scenarios for analysis of emissions, climate change, impacts, and response strategies. Technical summary, Noordwijkerhout, Netherlands.

Jadmiko, S.D., D. Murdiyarso, and A. Faqih. 2017. Koreksi bias luaran model iklim regional untuk analisis kekeringan. Jurnal Tanah dan Iklim, 41(1): 25-36. [in Indonesia]

Kudo, S., T. Sayama, A. Hasegawa, and Y. Iwami. 2015. Assessment of climate change impact on flood discharge and inundation in the Solo River Basin, Indonesia. Journal of Japan Society of Civil Engineers, Ser. B2 (Hydraulic Engineering), 59: 1321-1326.

Moriasi, D.N., J.G. Arnold, M.W. Van Liew, R.L. Bingner, R.D. Harmel, and T.L. Veith 2007. Model evaluation guidelines for systematic quantification of accuracy in watershed simulations. Trans ASABE 50(3): 885–900.

Moss, R.H., J.A. Edmonds, K.A. Hibbard, M.R. Manning, S.K. Rose, S.P. Van Vuuren, T.R. Carter, S. Emori, M. Kainuma, T. Kram, G.A. Meehl, J.F.B. Mitchel, N. Nakicennovic, K. Riahi, S.J. Smith, R.J. Stouffer, A.M. Thomson, J.P. Weyant, and T.J. Wilbanks. 2010. The next generation of scenarios for climate change research and assessment. Nature, 463: 747-756.

Mwangi, H.M., S. Julich, S.D. Pati, M.A. McDonald, and K.H. Feger. 2016. Relative contribution of land use change and climate variability on discharge of upper Mara River, Kenya. Journal of Hydrology: Regional Studies 5, 2016, 244–260.

Narulita, I., and W. Ningrum. 2018. Extreme flood event analysis in Indonesia based on rainfall intensity and recharge capacity. IOP Conf. Ser.: Earth Environ. Sci. 118: 012045.

Nash, J., and J.V Sutcliffe. 1970. River flow forecasting through conceptual models 1: A discussion of principles, J. Hydrol, 10: 282–290.

Nastitia, K.D., Y. Kima, K. Junga, and H. An. 2015. The application of Rainfall-Runoff-Inundation (RRI) model for inundation case in upper Citarum Watershed, West Java-Indonesia. Procedia Engineering, 125: 166 – 172.

Naylor, R.L., D. S. Battisti, D.J. Vimont, W.P. Falcon, and M.S. Burke 2007. Assessing risks of climate variability and climate change for Indonesian rice agriculture. Proceedings of the National Academy of Sciences of the United States of America, 104 (19): 7752–7757.

Nugroho, P., D. Marsono, P. Sudira, and H. Suryatmojo. 2013. Impact of landuse changes on water balance. Procedia Environ Sci., 17: 256–262.

Piani, C., J.O. Haerter, E. Coppola. 2010. Statistical bias correction for daily precipitation in regional climate models over Europe. Theoretical and Applied Climatology, 99(1–2): 187–192.

Ridwansyah, I., A. Sapei, and M. Raimadona. 2012. Applying SWAT to predict impact of landuse change on hydrological response in upper Cimanuk catchment area. In: The 5th international remote sensing and GIS workshop series on demography, land use-land cover and disaster, Bandung, Indonesia.

Ridwansyah, I., M. Yulianti , Apip, S. Onodera, Y. Shimizu, H. Wibowo, and M. Fakhrudin 2020. Limnology, 21: 487–498.

Sayama, T. 2017. Rainfall-Runoff-Inundation (RRI) Model User's Manual. International Center for Water Hazard and Risk Management (ICHARM), Public Works Research Institute (PWRI), Disaster Prevention Research Institute (DPRI), Kyoto University.

Sayama, T., G. Ozawa, T. Kawakami, D. Nabesaka, and K. Fukami. 2012. Rainfall–runoff–inundation analysis of the 2010 Pakistan flood in the Kabul River basin. Hydrological Sciences Journal, 57 (2): 298-312.

Sayama, T., Y. Tatebe, Y. Iwami, and S. Tanaka. 2015. Hydrologic sensitivity of flood runoff and inundation: 2011 Thailand floods in the Chao Phraya River basin. Nat. Hazards Earth Syst. Sci., 15: 1617-1630.

Tarigan, S., and A. Faqih A. 2019. Impact of changes in climate and land use on the future Streamflow fluctuation: case study merangin Tembesi Watershed, Jambi Province, Indonesia. Jurnal Pengelolaan Sumberdaya Alam dan Lingkungan, 9 (1): 181-189.

Thomas, V., and R. López. 2015. Global Increase in Climate-Related Disasters. Asian Development Bank, Philippines.

Thomson, A.M., K.V. Calvin, S. J. Smith, G.P. Kyle, A. Volke, P. Patel, S. Delgado-Arias, B. Bond-Lamberty, M.A. Wise, L. E. Clarke and J.A. Edmonds. 2011. RCP4.5: a pathway for stabilization of radiative forcing by 2100. Climatic Change, 109:77–94

Woldemichael, A.T., F. Hossain, R. Sr. Pielke, and A. Beltrán-Przekurat. 2012. Understanding the impact of dam-triggered land use/land cover change on the modification of extreme precipitation. Water Resource Res., 48(9): 1-6.

Xu, X., D. Yang, H. Yang, and H. Lei. 2014. Attribution analysis based on the budyko hypothesis for detecting the dominant cause of run off decline in Haihe basin. Journal of Hydrology 510 (2014): 530–540.

Yigzaw, W., and F. Hossain. 2016. Land use and land cover impact on probable maximum flood and sedimentation for artificial reservoirs: case study in the Western United States. J. Hydrol Eng., 21(2): 05015022.

Zhang, L., Z. Nan, Y. Xu, and S. Li. 2016. Hydrological impacts of land use change and climate variability in the Headwater Region of the Heihe River Basin, Northwest China. PLoS One. 2016 11 (6).